Journal of Materials Chemistry C

Accepted Manuscript

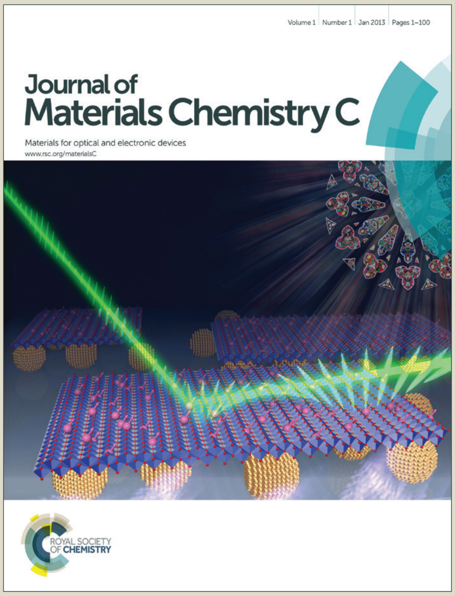

ROYAL SOCIETY OF CHEMISTRY

www.rsc.org/materialsC

Journal of Materials Chemistry C RSCPublishing

ARTICLE

Controlled roughness reduction of patterned resist polymers using laser-induced sub-millisecond heating

Cite this: DOI: 10.1039/x0xx00000x

Byungki Jung,[a] Christopher K. Ober[a] and Michael O. Thompson*[a]

Received 00th January 2012,
Accepted 00th January 2012

DOI: 10.1039/x0xx00000x

www.rsc.org/

High resolution polymer resist systems are critical for nanometer-scale photolithographic patterning. Substantial research has explored modifications in resist formulations and pattern development protocols to control critical dimensions (CD) and line width roughness (LWR), and post-development treatment of polymer patterns has also received active attention. In this work, we use a laser-induced heating technique (λ = 10.6 μm) to anneal (hardbake) fully developed polymer patterns at peak temperatures between 175-450 °C for 500 μs. Polymer flow at temperatures far above the glass transition (~100 °C) enables surface energy minimization to reduce pattern roughness. Results from this laser hardbake process are compared to conventional techniques using a vacuum-chuck hot plate at 90-150 °C for 30 s. At low temperatures, surface roughness can be reduced only with unacceptable loss of the sidewall angle and trench profiles. In contrast, reductions in LWR (from 6.4 nm to 2.6 nm) and surface roughness of 35% are achieved with less than 1 nm change in CD for a common acrylate-based polymer under the laser hardbake at elevated temperatures. Minimal changes in the sidewall angle and trench profiles are observed due to nano-scale flow over the sub-millisecond time frames. This novel sub-millisecond heating technique provides a means to reduce roughness by surface energy minimization in high resolution polymer patterns with minimal resolution loss, potentially complementing other advances in high performance photolithography.

1. Introduction

For over 40 years, photolithography has been a key driver for advances in microelectronics, leading to faster and more efficient computing. At the most basic level, photolithography involves patterning a radiation-sensitive polymer which acts as a stencil for underlying films during subsequent etching steps.[1,2] Most chemically amplified photoresist patterning using deep ultraviolet (DUV) and extreme UV (EUV) light sources involves radiatively generating a strong acid in the resist film which cleaves (deprotects) esters along the polymer backbone during a subsequent heating step known as the post-exposure bake (PEB). This modifies the resist solubility enabling selective removal with a developing solvent.[1-4] Although resist materials and their patterning chemistries continue to evolve to achieve ever higher resolutions, key concerns remain for controlling critical dimension (CD) and line width roughness (LWR) of developed patterns. For 11 nm half-pitch resolutions, the International Technology Roadmap for Semiconductors (ITRS) suggests a control of CD and LWR to less than 1.0 nm and 0.9 nm (3σ) respectively.[5] Research to date has focused primarily on improving the pattern resolution during UV exposure,[6-7] post-exposure bake,[8,9] and development.[10-12] In parallel, processes to improve resist metrics after development are also being actively explored.[13-14]

An ideal post-develop process would reduce LWR without modifying the CD and pattern profile (sidewall angle). Processes that have been previously explored to reduce LWR after development include chemical rinsing, smoothing by vapor-induced melting of the resist surface, smoothing by resist flow using additional heating (hardbake), and controlled etching of the resist surface.[13-16] While these processes have demonstrated reduced roughness, significant changes in the CD and pattern profiles were observed due to the swelling of the polymer and/or loss in resist thickness. Smoothing by polymer flow using a 10-30 s hardbake above the resist's glass transition temperature (T_g), for example, reduced the LWR up to 15% but excessive flow in the lateral direction changed the profile dimension and the sidewall angle from its original form.[13,17] If the heating duration could be minimized and controlled to prevent excessive flow of the resist polymer while maintaining the thermal budget required to induce polymer flow, an ideal post-develop technique might be established.

Conventional heating methods using furnace or vacuum-chuck hot-plate involve heating substrates in the seconds time frame with temperature ramp rates on the order of 10-100 K/s. In contrast, continuous wave (CW) laser heating sources can transiently heat thin polymer films above their T_g's in sub-millisecond time frame at 10^4-10^5 K/s to peak temperatures

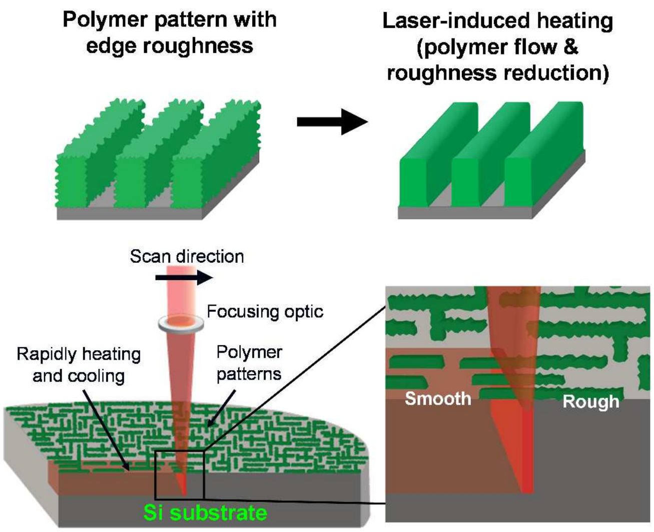

Fig. 1 Schematics of laser-induced resist hardbake process. Patterned resist polymers are heated using a scanned line-shaped laser. When heated above the glass transition temperature, the polymer flows and minimizes the surface energy to reduce pattern roughness.

well beyond normal polymer decomposition temperatures.[8,18] This process, known as laser spike annealing (LSA), was first utilized as a millisecond annealing technique to activate dopants while minimizing diffusion in ultra-shallow semiconductor junctions.[19,20] In LSA (Fig. 1), a line-focused CW laser is scanned over the substrate to rapidly heat the surface for microseconds to milliseconds, after which cooling occurs rapidly by thermal conduction into the substrate. In this work, LSA was used to anneal fully developed resist patterns at temperatures of 295-450 °C for 500 µs. Under these conditions, the patterned polymer is expected to flow to minimize the total surface energy resulting in a reduction of LWR without damaging the sidewall angle and CD, as shown schematically in Figure 1. Previously, we demonstrated the feasibility of this technique using an acrylate-based EUV resist polymer.[21] LWR reductions up to 30% were observed prior to significant changes to CD. In this paper, we investigate the general applicability of the technique on a range of resist structures, and directly compare the LWR changes to heating by conventional hot-plate methods at lower temperature for seconds time frame. Roughness reduction using this laser technique may ultimately enable the controlled reflow of organic polymers in nanometer-scale surface patterning that will complement high resolution patterning.

2. Experimental Section

2.1 Laser spike annealing as a hardbake method and temperature calibration

Laser spike annealing (LSA) was initially developed as a sub-millisecond annealing technique for shallow junctions in the semiconductor industry. In this work, a CO_2 laser with a wavelength of 10.6 µm was focused to a 90 µm by 700 µm line. The heating duration (dwell time), defined as the full width half maximum (FWHM) of the beam divided by the scan velocity, approximates the time at which the sample experiences the peak temperature. Figure 2a shows a measured surface temperature profile as a function of time at 20 W for a 500 µs dwell. Heavily doped wafers (p type resistivity ~0.015 Ω·cm) were used to ensure full absorption of the CO_2 laser wavelength through intraband free carrier absorption. Temperatures in the top micron of the surface are essentially isothermal, with temperatures decaying over a 200 µm length scale into the bulk of the sample. Consequently, for the 35-50 nm resist films in this work, temperature variations through the thickness of the film are expected to be less than 1 °C.

Silicon substrate temperatures using the CO_2 beam were measured using platinum resistors (thermistors), which were calibrated to experimental measurements of gold and Si melting temperatures.[18] 50 nm thick thermistors with total area $<10^{-5}$ cm^2 were fabricated to measure the resistance change during CO_2 scans at varying laser powers. The resistance change is directly proportional to temperature and established the shape of the temperature versus laser power curve. Absolute temperatures were assigned from the experimentally observed melting of Si (1414 °C) or micron-size gold dots (1064 °C). The calibration from power to temperature is shown in Figure 2b.

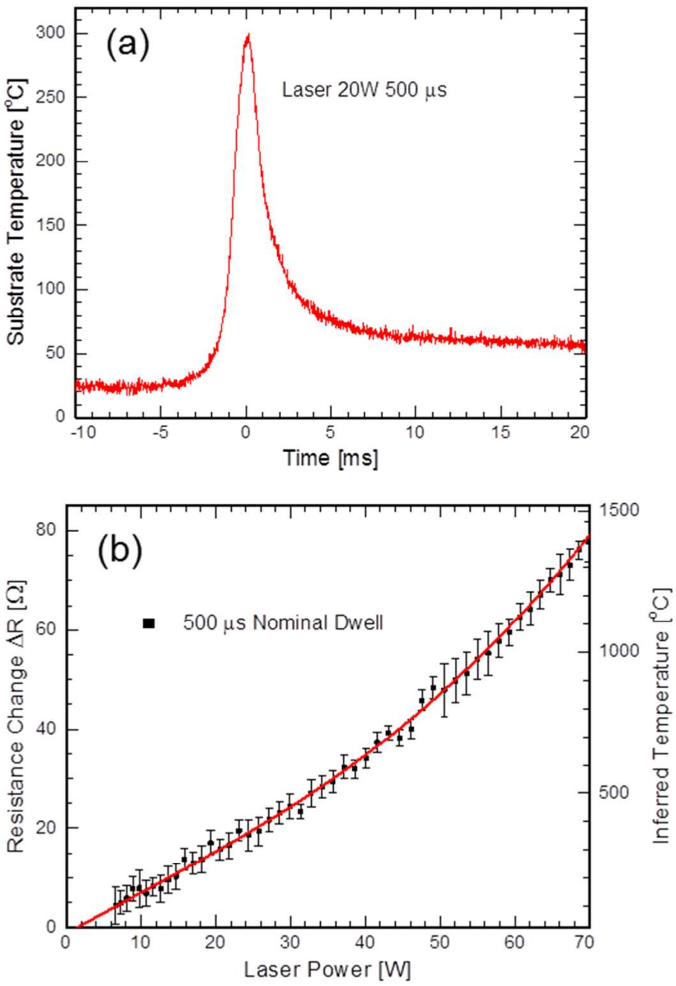

Fig. 2 Characterization of the millisecond heating method using a CO_2 laser system and platinum resistors (thermistors). (a) Measured temporal profile during a scan at 20 W for 500 µs corresponding to a substrate peak temperature of 300 °C. (b) Measured peak temperature as a function of laser power for a 500 µs dwell. Absolute temperatures are calibrated to the melting of Si and gold.

2.2 Materials

Three commercially available resist polymers were spun on Si wafers with target thicknesses of 35-50 nm and exposed at EUV (13.5 nm) wavelengths. The investigated systems included an acrylate based resist platform (referred to as acrylate-based polymer) where the deprotection mechanism during PEB converts esters along the polymer backbone into carboxylic acids, and two hybrid polymers (such as copolymers containing both poly(hydroxy styrene) and acrylates) that are expected to be sensitive to hardbake temperatures (referred to as hybrid polymer A and hybrid polymer B).[22] All three polymers had reported glass transition temperatures (T_g) near 100 °C as specified by the supplier. After EUV exposure, samples underwent conventional hot-plate PEB under optimal conditions and were developed in tetramethylammonium hydroxide (TMAH, 0.26 N). The developed patterns, 30 nm lines and spaces, were subsequently hardbaked using either a hot-plate at 90-150 °C for 30 s or by LSA at 175-450 °C for 500 µs. Original and hardbaked patterns were imaged using SEM and AFM to quantify CD, LWR, and surface roughness.

2.3 Pattern characterization methods

Following either hot-plate or laser-induced hardbake, resist patterns containing 30 nm lines/spaces were imaged using a Leo 1550 FESEM with constant magnification of 200k. SuMMIT[23] was used to quantify the critical dimension (CD) and line width roughness (LWR) from a minimum of eight lines from a single SEM image. For consistency, SEM images of the original and hardbaked patterns were obtained from adjacent areas to minimize systematic variations across the wafer. At least five SEM images were analyzed at a given hardbake condition to average the CD and LWR values. In this work, LWR is characterized as the 3σ deviation of the line edge from a straight line, with each line measured over a 375 nm length.

To visualize the resist profile and to quantify the surface roughness, resist profiles were measured by an AFM (Dimension Icon by Bruker). In order to image the extremely high aspect ratio photoresist profiles, carbon nanotube tips with diameters less than 15 nm and heights greater than 150 nm were obtained from K-TEK Nanotechnology LLC. These high resolution tips were designed specifically for measuring high aspect ratio trenches.

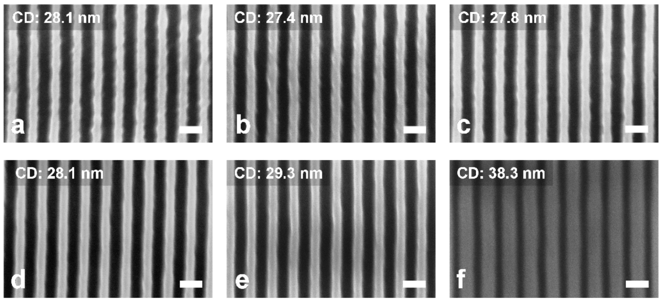

Fig. 3 SEM images of 30 nm line/space patterns generated in the hybrid polymer A followed by laser-induced hardbake for 500 µs. Images show (a) the original pattern, and patterns after heating to (b) 235 °C, (c) 295 °C, (d) 355 °C, (e) 385 °C and (f) 420 °C. While the original pattern shows significant roughness on line edges, resist smoothing through polymer flow is observed for increasing hardbake temperatures. At 420 °C however, excessive flow is apparent as the CD is significantly changed. All scale bars correspond to 60 nm.

3. Results and discussion

Figure 3 shows SEM images of hybrid polymer A after LSA processing at 225-420 °C. While the unannealed pattern shows significant roughness on the edges, smoothing is readily apparent as the hardbake temperature increases. Once the laser hardbake temperature reaches 420 °C, however, excessive polymer flow is observed in the lateral direction, changing both CD and the sidewall angle.

This smoothing behavior was observed in all three of the investigated resist systems. The acrylate-based polymer and hybrid polymer B exhibited similar smoothing beyond a material-dependent threshold temperature (Figure 4 and Supplementary Information). In all three systems, the initial LWR was between 5.3 and 6.4 nm, which decreased to 2.6 and 3.1 nm following laser hardbake. Corresponding changes in CD were less than 1 nm. However, the optimal temperature for smoothing is strongly dependent on polymer structure, increasing from 325 °C for hybrid polymer B to 385 °C for the acrylate-based resist. To first order, this temperature would be expected to scale with the glass transition of the resist system.

Quantitative changes in CD and LWR as a function of laser hardbake temperature are shown in Figure 5 for all three polymer systems. To remove systematic variations in CD and LWR over the wafer, the same features were measured before and after hardbake. This enabled absolute determination of

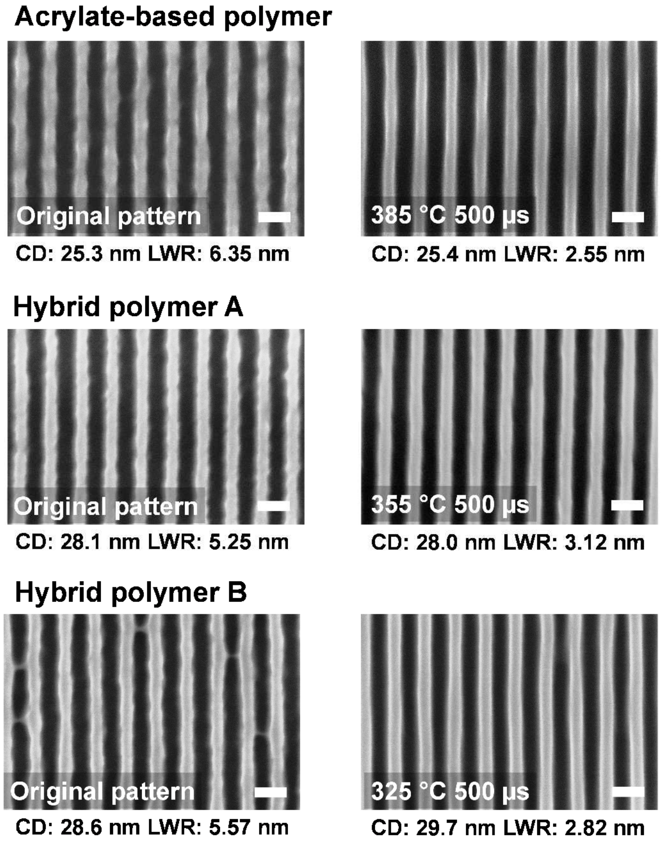

Fig. 4 SEM images of 30 nm line/space patterns before and after laser hardbake at optimal heating conditions for three investigated resist systems. For all investigated resist systems, line width roughness is reduced up to 60% with less than 5% change in critical dimension. All scale bars correspond to 60 nm.

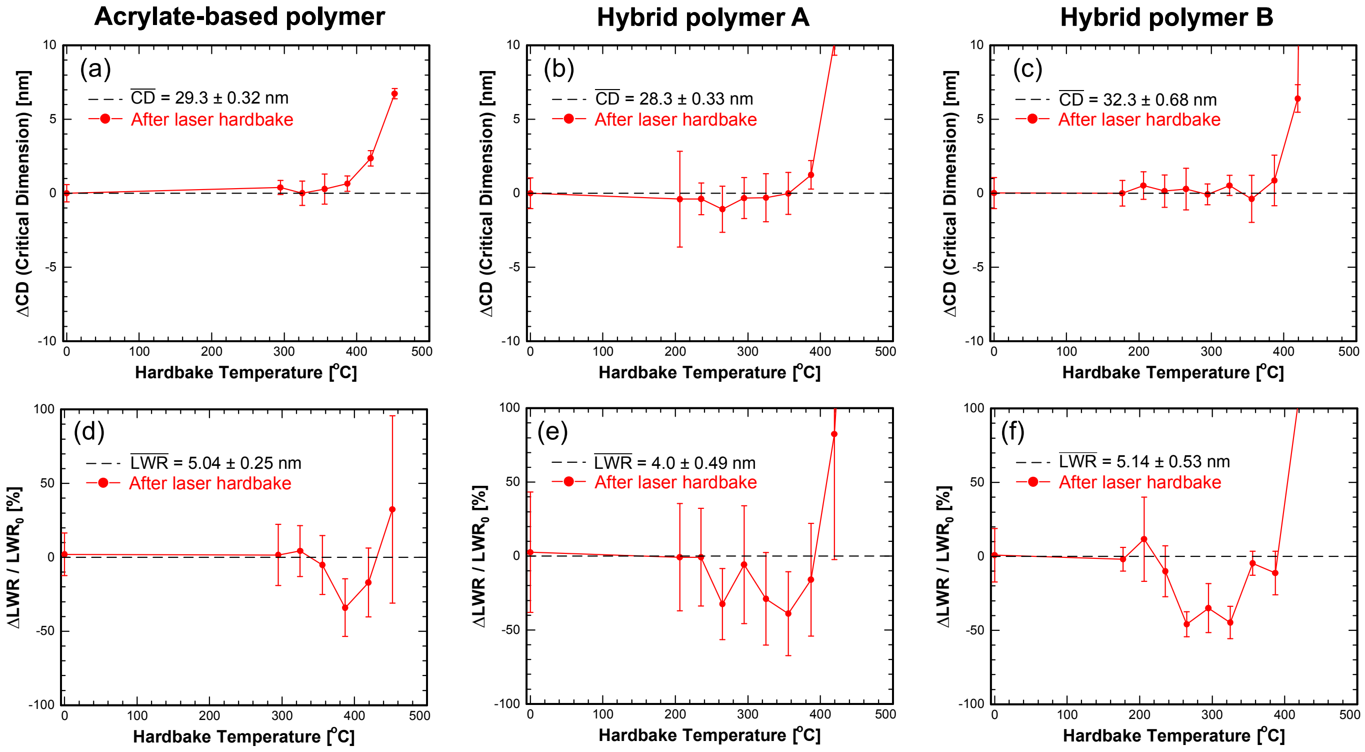

Fig. 5 Quantitative changes in critical dimension (a, b, c) and line width roughness (d, e, f) as a function of laser hardbake temperature for three investigated resist polymers. For all polymers, a favorable trade-off between LWR reduction up to 40 % and CD change less than 2 nm occurs at temperatures where polymer flow is optimized and controlled. Laser hardbakes were performed at $\tau_{\mathrm{dwell}} = 500$ µs.

ΔCD and ΔLWR independent of fluctuations unrelated to the hardbake. Pre-hardbake variations in CD were less than ±1 nm and LWR less than ±0.5 nm over all examined features. Uncertainties (error bars) in ΔCD and ΔLWR represent variations between at least five SEM images, each consisting of eight lines and spaces.

Changes in CD are quantified in Figures 5a, 5b, and 5c. Independent of the resist system, the CD changed by less than 1 nm for temperatures up to 385 °C with a 500 µs dwell. Large changes were only observed as temperatures exceeded 420 °C. At these higher temperatures, CD increases rapidly as the original profiles deteriorate due to polymer flow. Figures 5d, 5e, and 5f show changes in LWR over the same conditions. As expected, no changes are observed at the lowest temperatures. For the acrylate-based polymer, LWR is unchanged to 320 °C, but decreases to a minimum of 2.6 nm (a 35% decrease) at 385 °C before increasing rapidly above 450 °C. The two hybrid systems show no LWR change to 235 °C, followed by a broad reduction in LWR up to 385 °C, and finally a large increase in LWR above 420 °C. For hybrid polymer A, the maximum LWR decrease is 30-40% to 3.1 nm. Hybrid polymer B shows a similar broad minimum in LWR with decrease of 40-50% to 2.6 nm. At the optimum heating temperatures, individual samples showed up to a 60% reduction in LWR after the sub-millisecond laser hardbake.

The optimal temperatures for LWR reduction with minimal change in CD occur at 385, 355, and 325 °C for the acrylate-based polymer, hybrid polymer A, and hybrid polymer B respectively. At these temperatures, the polymer's viscosity decreases sufficiently to flow on nanometer scales within the 500 µs time frame enabling smoothening by surface energy minimization, but with insufficient time to incur flow over larger dimensions. Increasing the hardbake temperature above 420 °C reduces the viscosity to a level where flow occurs rapidly over these larger dimensions resulting in a drastic increase in both CD and LWR. While these critical temperatures are significantly higher than the T_g of all three polymers (~100 °C), the increase is not surprising as the five orders of magnitude decrease in heating duration compensates the lower viscosity. In previous research, a similar shift in another thermal threshold was observed for decomposition of an acrylate-based resist system, increasing by 400 °C above its conventional limits from seconds to sub-millisecond time frames.[8]

The optimum hardbake temperature for these three polymer systems were between 325 °C and 385 °C. However, while CD is not significantly changed, even short range flow may modify the resist sidewall angle and impact subsequent etch processes. AFM analysis of the resist profiles was used to evaluate changes in the local resist topography. Figure 6 shows AFM images of the acrylate-based resist measured after hardbake at varying hot-plate and laser temperatures. Features in these images are 80 nm wide trenches separated by 320 nm, permitting AFM tip access to resolve line edge features and providing large areas to assess surface roughness. Figure 5a shows typical original patterns prior to any thermal processing. Under hot-plate hardbake (Figures 6b and 6c), the bottom of the trench collapses toward a v-shape profile at both 90 °C and 115 °C for 30 s. Although some surface roughness reduction is apparent at both temperatures, thinning of trenches (CD loss) is

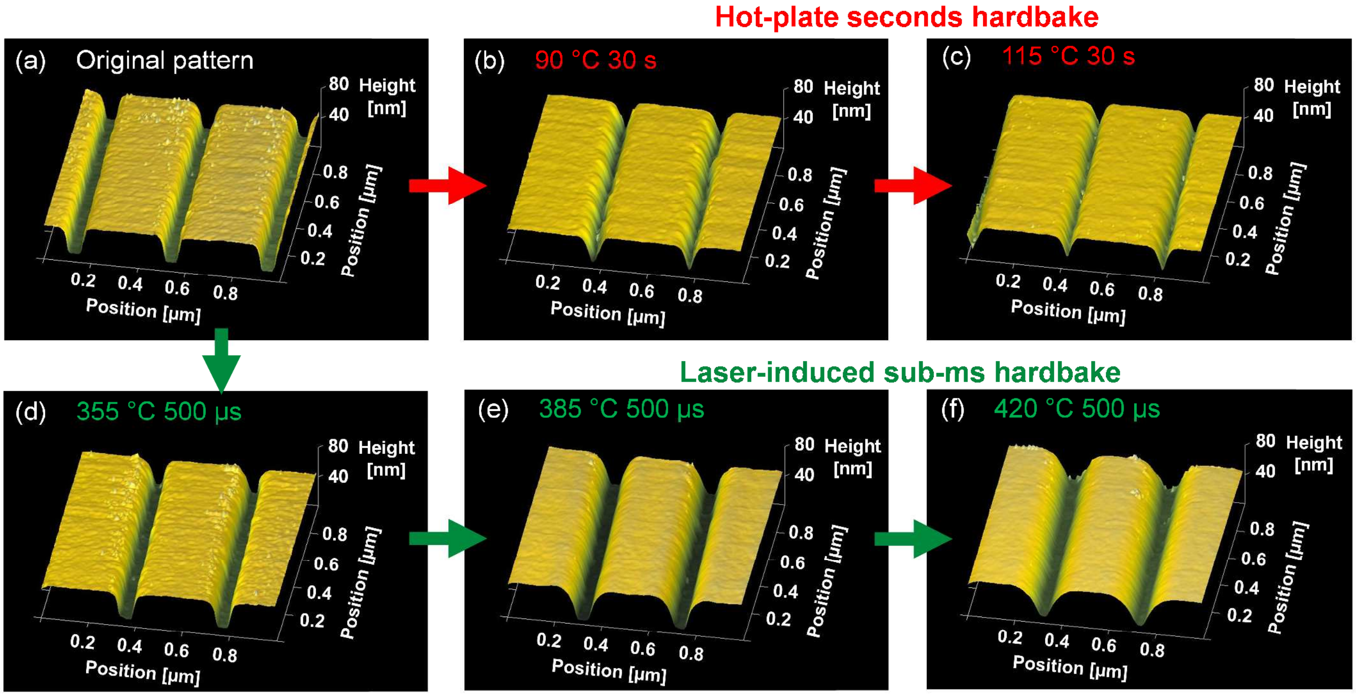

Fig. 6 Resist profiles obtained from AFM measurements as a function of hardbake temperature using the acrylate-based polymer showing (a) the original pattern, (b, c) hot-plate hardbake at 90 °C and 115 °C for 30 s, and (d, e, f) laser hardbake at 355 °C, 385 °C, and 420 °C for 500 µs respectively. While surface roughness is reduced for both hardbake methods, trenches remain intact only for the laser-induced sub-millisecond anneal.

very significant and the sidewall profile is almost lost. These results are consistent with previous results and trends observed using conventional hardbake in the seconds time frames.[13,17,24,25] For sub-millisecond hardbake however, there are only minimal changes in the trench profile below 385 °C. At 385 °C, the critical temperature for the acrylate based polymer, the surface roughness has largely disappeared with only minimal rounding of the sidewall angle. Smoothing of the sidewalls and near the bottom of the trench was also observed, but the bottom of the trenches remained well defined with minimal change. As the hardbake temperature is increased further to 420 °C, significant loss of the sidewall angle due to flow is readily apparent even for the 500 µs laser-induced heating.

Profiles of the resist height as a function of position for these trenches are shown in Figure 7 for the original pattern, hot-plate hardbake at 90 °C, and laser hardbake at 385 °C. Loss of the sidewall angle and the CD is most severe under hot-plate processing, with complete loss of the trench bottom. Resist flow in this case occurs predominately in the trenches with much less change on the surface of the resist patterns. In contrast, the laser hardbake shows primarily surface flow, surface smoothing, and corner smoothing with minimal damage in the trench profile where the change is limited to the top 15 nm of resist. As a resist stencil for the subsequent etching step, the profile after laser hardbake remains viable while the CD loss using hot-plate hardbake would be problematic.

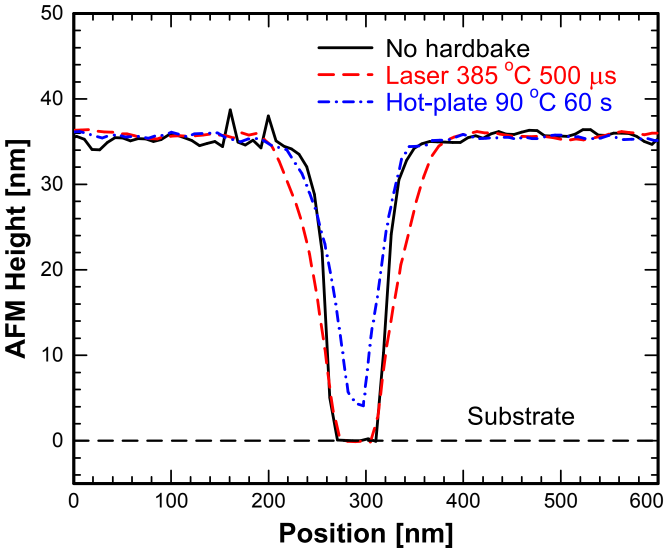

Fig. 7 Comparison of AFM trench profiles in the acrylate-based resist polymer. Traces are shown for the original profile prior to hardbake, hot plate hardbake at 90 °C for 30 s, and laser hardbake at 385 °C for 500 µs.

To characterize the surface roughness reduction, quantitative measures were obtained from arbitrary but consistent areas (100 nm by 850 nm on the resist surface) in the AFM images. Table 1 summarizes the average roughness (R_a), root mean square (RMS) roughness (R_q), and maximum roughness (R_{max}) for hot-plate and laser hardbake. Using hot-plate hardbake, a minimum in all three measures was observed at temperatures between 90 °C and 115 °C. While R_q was reduced up to 45% at 115 °C, this reduction is not useful given the collapse of the sidewall profiles. As temperature is increased further, instabilities in the resist rapidly increase the roughness which ultimately approaches and exceeds the initial values. Under laser hardbake, similar reductions in R_q up to

Table 1 Surface roughness measurements of the acrylate-based resist pattern showing the average roughness, root mean square roughness, and maximum roughness (R_a, R_q, and R_{max} respectively) as a function of hardbake temperature using a) hot-plate or b) laser-induced heating.

(a) Hot-plate 30 s	Surface roughness [nm]		
Temperature [°C]	Average (R_a)	RMS (R_q)	Max (R_{max})
No anneal	0.40	0.62	9.46
90	0.30	0.37	2.32
115	**0.26**	**0.34**	**3.60**
130	0.35	0.50	4.91
150	0.59	0.84	7.01

(b) Laser 500 µs	Surface roughness [nm]		
Temperature [°C]	Average (R_a)	RMS (R_q)	Max (R_{max})
No anneal	0.39	0.62	9.46
355	0.35	0.45	3.58
385	**0.31**	**0.38**	**2.54**
420	**0.29**	**0.37**	**1.29**

40% are observed at 385 °C. At this temperature, however, the trench profiles remain essentially intact. With increasing laser hardbake temperature, all roughness measurements continue to decrease which suggest increasing polymer flow during the 500 µs heating with no instabilities. The large decrease, up to 75% in R_{max} for both hardbake methods, is due to the loss of the sharp bumps (up to 10 nm in height) initially present on the surface. Removal of such high spatial frequency roughness is expected to occur first as the resist viscosity decreases exponentially with temperature (see Supplementary Information). Collectively, these data indicate that the acrylate-based polymer is more sensitive to large scale flow and profile damage during the seconds hardbake as compared with the sub millisecond hardbake at higher temperatures.

The CD and LWR measurements by SEM indicate an optimal laser hardbake temperature between 325 °C and 385 °C for the three investigated polymer systems. For the acrylate-based polymer at 385 °C, LWR is reduced up to 30% with less than 1 nm change in CD, and with R_a and R_q reduced by 21% and 38% respectively. As both LWR and surface roughness reductions are governed by viscous polymer flow, reductions between these two values are expected to be correlated as observed. As the temperature is increased above T_g (~100 °C), the reduced viscosity of the polymer enables flow to minimize surface energies reflected in both LWR and the surface roughness reductions. With viscosity decreasing rapidly with temperature, the temperature range for hardbake is relatively narrow for surface smoothing before appreciable loss of CD and sidewall angle.

It is somewhat surprising that, under laser heating, significant polymer flow occurs on the sidewall at intermediate temperatures (325-400 °C) to reduce LWR while minimal macroscopic flow occurs to change the CD. Fundamentally, both CD and LWR changes arise from the same reduction in the resist viscosity and hence their behavior should be comparable. Experimentally under laser heating, however, there is almost a 100 °C difference between the onset of flow for LWR reduction and bulk flow resulting in CD loss. This implies an underlying difference in the resist behaviors on the sidewalls (impacting LWR) and in the bulk (impacting CD). But there is also a difference between the laser and hot plate regimes; while data show a 100 °C window under laser heating, polymer flow in the trenches occurs at the same temperature as LWR reduction for hot-plate heating which results in a very limited process window.

There are several potential origins for these differences. First, polymer on the sidewalls will be chemically different compared to the bulk polymer due to partial deprotection during PEB and pattern development. For the acrylate-based polymer, this corresponds to higher concentrations of carboxylic acids and fewer thermally stable carbonyl esters on the polymer backbone. These changes would act to lower T_g in the sidewall resist. This does not, however, explain the laser hardbake data. Resist on the surface would be chemically identical to the bulk, but AFM shows R_a reductions occurring in the same temperature range as LWR reductions. Equally, a reduced T_g on the sidewall would tend to enhance LWR reductions under hot-plate heating instead. A second origin may be related to plasticization of the sidewalls and surface by residual solvents after development. On hot-plate seconds time frame, these solvents would have time to evaporate leaving minimal chemical differences between the sidewall and resist bulk. In contrast, the sub-millisecond time frame of laser heating may kinetically suppress this evaporation resulting in enhanced flow in both the plasticized sidewalls and surfaces. Finally, the effect may be related to polymer flow at the trench bottom out of the resist, substrate, and vapor triple junction. Changes in the delicate balance between surface energies at the polymer/substrate interface and the polymer/vapor interface may delay wetting or effectively pin this boundary preventing collapse of the trench profiles on sub-millisecond time frames. Further studies of the flow behavior over varying time frames and conditions are necessary to resolve this issue.

4. Conclusions

Laser-induced sub-millisecond heating is introduced as a post-develop process for controlling and minimizing LWR with minimal CD loss. Three different polymers were patterned and subjected to laser hardbake at peak temperatures between 175 °C and 450 °C for 500 µs. Results were compared with conventional hot-plate hardbake performed at temperatures between 90 °C and 150 °C for 30 s. For both heating methods, pattern smoothing due to polymer flow above T_g was observed. At the optimal laser heating conditions, LWR was reduced by 35% on an acrylate-based polymer with less than 1 nm change in CD. Surface roughness was also decreased up to 40% with minimal change to the sidewall angle. No significant change in LWR was observed under hot-plate heating before deteriorations in CD and the sidewall angle. These data demonstrate the potential for a sub millisecond laser-induced heating to address some of the roughness challenges in organic patterns beyond resist polymers, and provides a means to compliment high resolution patterning through nano-scale flow and surface energy minimization.

Acknowledgements

We would like to gratefully acknowledge Manish Chandhok (Intel Corporation) for helpful discussion. K-TEK Nanotechnology LLC (Ruben Martinez and Steve Shim) is thanked for providing the high resolution AFM (CDI) probes. This work made use of facilities in the Cornell Center for Materials Research (NSF-DMR 0520404) and the Cornell Nanoscale Science and Technology Facility (NSF-ECS 0335765). Work at Cornell University was supported by Intel Corporation.

Notes and references

[a] Department of Materials Science and Engineering, Cornell University, Ithaca, NY 14853, USA. E-mail: mot1@cornell.edu

Electronic Supplementary Information (ESI) available: Additional SEM images showing LWR reduction on two additional polymer systems and power spectral densities are also included. See DOI: 10.1039/b000000x/

1 H. Ito, *Adv. Polym. Sci.*, 2005, **172**, 27.

2 H. Ito and C. G. Willson, *Polym. Eng. Sci.*, 1983, **23**, 1012.

3 W. H. Zhou, S. M. Kuebler, K. L. Braun, T. Yu, J. K. Cammack, C. K. Ober, J. W. Perry and S. R. Marder, *Science*, 2002, **296**, 1106.

4 G. M. Wallraff and W. D. Hinsberg, *Chem Rev.*, 1999, **99**, 1801.

5 Semiconductor Industry Association, The International Technology Roadmap for Semiconductors, Washington, DC, USA, 2013, http://www.itrs.net.

6 T. Ito and S. Okazaki, *Nature*, 2000, **406**, 1027.

7 D. Bratton, D. Yang, J. Dai and C. K. Ober, *Polym. Adv. Technol.*, 2006, **17**, 94.

8 B. Jung, J. Sha, F. Paredes, M. Chandhok, T. R. Younkin, U. Wiesner, C. K. Ober and M. O. Thompson, *ACS Nano*, 2012, **6**, 5830.

9 W. D. Hinsberg, F. A. Houle, M. I. Sanchez and G. M. Wallraff, *IBM J. Res. Dev.*, 2001, **45**, 667.

10 D. L. Goldfarb, J. J. de Pablo, P. F. Nealey, J. P. Simons, W. M. Moreau and M. Angelopoulos, *J. Vac. Sci. Technol. B*, 2000, **18**, 3313.

11 W. Hu, K. Sarveswaran, M. Lieberman and G. H. Bernstein, *J. Vac. Sci. Technol. B*, 2004, **22**, 1711.

12 A. I. Cooper, *Adv. Mater.*, 2001, **13**, 1111.

13 M. Chandhok, K. Frasure, E. S. Putna, T. R. Younkin, W. Rachmady, U. Shah and W. Yueh, *J. Vac. Sci. Technol. B*, 2008, **26**, 2265.

14 A. V. Pret, R. Gronheid and P. Foubert, *J. Micro/Nanolith. MEMS MOEMS*, 2010, **9**, 041203.

15 O. Miyahara, K. Tanaka, S. Wakamizu, J. Kitano and Y. Yamada, *Proc. SPIE*, 2004, **5376**, 830.

16 P. Zhang, M. Jaramillo, S. Cassel, T. Wallow, A. Acheta, A. R. Pawloski, S. Bell and R. H. Kim, *Proc. SPIE*, 2006, **6153**, 61533Y.

17 M. Padmanaban, D. Rentkiewicz, S. Lee, C. Hong, D. Lee, D. Rahman, R. Sakamuri and R. R. Dammel, *Proc. SPIE* 2005, **5753**, 862.

18 K. Iyengar, B. Jung, M. Willemann, P. Clancy and M. O. Thompson, *Appl. Phys. Lett.*, 2012, **100**, 211915.

19 S. Talwar, D. Markle and M. Thompson, *Solid State Technol.*, 2003, **46**, 83.

20 T. Yamamoto, T. Kubo, T. Sukegawa, E. Takii, Y. Shimamune, N. Tamura, T. Sakoda, M. Nakamura, H. Ohta, T. Miyashita, H. Kurata, S. Satoh, M. Kase and T. Sugii, *Int. Elec. Devices Meet.* 2007, **1**, 143.

21 B. Jung, C. K. Ober, M. O. Thompson and M. Chandhok, *Proc. SPIE*, 2011, **7972**, 79722S.

22 E. S. Putna, T. R. Younkin, M. Chandhok and K. Frasure, *Proc. SPIE* 2009, **7273**, 72731L.

23 M. D. Shumway, P. Naulleau, K. A. Goldberg and J. Bokor, *J. Vac. Sci. Technol. B*, 2005, **23**, 2844.

24 B. J. Rice, H. B. Cao, M. Chandhok and R. P. Meagley, *Proc. SPIE* 2003, **5039**, 384.

25 R. Peters, K. Lucas, J. L. Cobb, C. Parker, K. Patterson, R. McCauley, M. Ercken, F. Van Roey, N. Vandenbroeck and I. K. Pollentier, *Proc. SPIE*, 2003, **5038**, 1311.